The structure polymer/As-Se-S doped by Bi for X-ray imaging

A. Chirita[a*], A. Hustuc[b], N. Nasedchina[a], S. Vatavu[a]
[a]*Semiconductors Physics and Devices Laboratory, Physics and Engineering Faculty, Moldova State University, Chisinau, Republic of Moldova*
[b]*Alarad SRL, Chisinau, Republic of Moldova*

The polymer/67at %$(As_2S_3)_{0,985}(Bi_2Se_3)_{0,015}$:33 at.% As_2Se_3 structure for X-ray imaging has been investigated. The possibility of registering relief-phase images for radiation of "white" spectrum of tungsten anode X-ray tube was shown.

(Received July 23, 2023; Accepted November 6, 2023)

Keywords: X-ray imaging, Chalcogenide glassy semiconductors, Thermoplastic

1. Introduction

Chalcogenide glassy semiconductors (CGS) of As-Se-S system exhibit a large implementation range, including optical information recording applications. CGS are sensitive materials to surface relief formation (mass-transport effect) under laser illumination [1-2], electron-beam recording [3-5], photoinduced transformation (photodarkening, photorefraction) [6-8], and as photoresist materials sensitive in UV-visible regions [9]. The photo-thermoplastic carriers, based on CGS [10], have high values of resolution power - up to 4000 mm^{-1} [11], diffraction efficiency - up to 40% [12], and 1–3 s real-time image formation [13]. The As_2S_3 thin films, as photoresists for X-ray photolithography, were investigated in [14-15]. The maximum sensitivity of As_2S_3 for X-ray photolithography is in the spectral range of 2-7 nm [14]. The use of As_2S_3 thin films as photoresists in the wavelength range of 0,1-0,6 nm requires large exposure times due to their low sensitivity in this spectral range. The polymer/As-Se-S-Sn structure to be used for X-ray imaging is presented in [16], showing the As-Se-S-Sn system X-ray sensitivity (λ=0,154 nm). The same studies were care out for the polymer/ As-Se-S-Te structure in [17]. This work aimed the investigations on Bi-doped As-Se-S chalcogenide glassy semiconductors for X-ray imaging applications.

2. Experimental setup

The carriers for X-ray imaging (Fig.1a) were obtained as a multilayer structure using vacuum technologies [18-19]: the flexible polyethylene terephthalate film (PET) substrate (1) was covered with a semitransparent chrome electrode (2), the sensitive layer (3) based on 67at%$(As_2S_3)_{0,985}(Bi_2Se_3)_{0,015}$:33at.% As_2Se_3 with a thickness of 4,2 μm was deposited onto the metal electrode, and the0,6 μm thick thermoplastic layer of polyepoxypropylcarbazole (4) was deposited onto the semiconductor layer.

* Corresponding author: arc_chirita@yahoo.com
https://doi.org/10.15251/CL.2023.2011.803

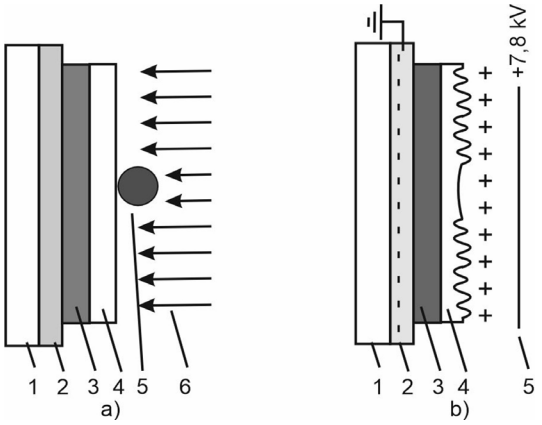

Fig. 1 a) 1. Polyethylene terephthalate film, 2. Chrome electrode, 3.Semiconductor layer of 67at%$(As_2S_3)_{0,985}(Bi_2Se_3)_{0,015}$:33at.% As_2Se_3, 4. Thermoplastic layer, 5. Microwire, 6. X-ray beam; b) Visualization of recorded image.

The X-ray setup based on a W tube (voltage 50 kV, current 50 mA) was used for sample irradiating. The samples were studied under continuous X-ray spectrum irradiation of the (also called "white" spectrum). The 447 nm monochromatic laser radiation was used for registration in the visible spectral regionp. The wires, having a diameter of starting from 30 μm down to 6 μm were used as masks for X-ray image recording. The wire was placed onto the surface of the thermoplastic layer (5, Fig.1a) and irradiated with X-ray or visible irradiation (6). The carrier is removed from the X-ray chamber after irradiation for the next step of image visualization [16-17, 20]. After irradiation, the carrier is heated up to a viscous state of the thermoplastic layer ($T=78^0C$) in the dark and charged for 2,5-3,2 s by use of high voltage (7,8 kV) corona charging (Fig.1b) [16-17]. The surface of the thermoplastic layer is charged with positive air ions (Fig.1b). As it was shown in [16-17], the conductivity of the semiconductor layer in the irradiated areas is higher due to the change in resistivity under irradiation. A relief-phase image of the registered object is being formed under the Coulomb interaction between positive charges on the surface of thermoplastic and negative charges in the semiconductor layer. The interaction between charges causes deformations of the thermoplastic layer in irradiated areas [10].

3. Results

The polyepoxypropylcarbazole was used as the thermoplastic layer in these experiments, unlike the studies presented in [16-17], where butylmetacrylate-styrene was used. Polyepoxypropylcarbazole has a higher plasticity compared to butilmetacrylate-styrene, which increases the resolution of the photothermoplastic process [21-22]. Fig.2a shows the microscope image of two crossed tungsten wires with a diameter of 30 μm which were used as masks (5, Fig.1). The image was recorded using the continuous spectrum of tungsten X-ray tube (absorbed dose 1,82 Gy). Thermoplastic visualization (Fig.1b) was carried out at a temperature of $T=78^0C$ and charging time t=3,2 s. After the visualization, the images were studied by use of an optical microscope in reflected light (1200^x magnification).

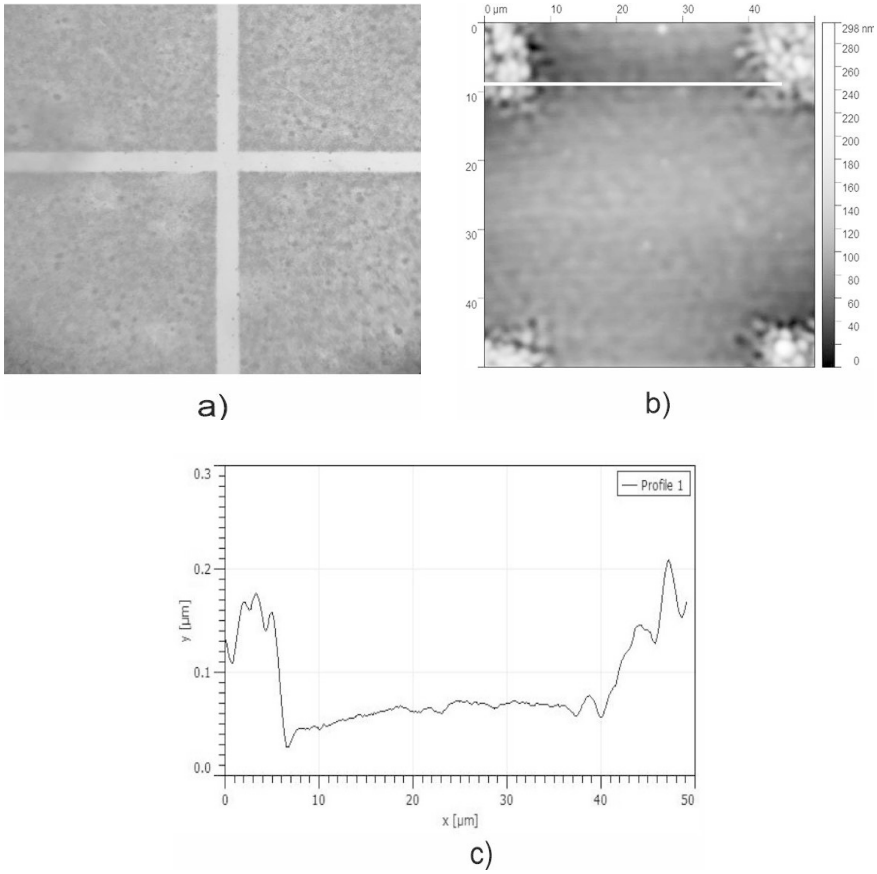

Fig.2 a) Microscopic image of tungsten wires with a diameter of 30 µm, b) AFM image of the wires crossing area, c) Thermoplastic deformation profile

The thermoplastic process forms a negative image of the initial object, due to the deformation of the thermoplastic layer in irradiated areas. A part of the image (crossed wire area) was investigated using the Atomic Force Microscopy (AFM) (Fig.2b). The selected part of the image covers both irradiated and non-irradiated areas. The surface profile (longitudinal white line along the image) shows an approximately 0,1 µm average depth considering irradiated and no irradiated areas (Fig.2c).

As a comparison (to X-rays) tool, carriers were investigated for visible light imaging. Similar to the previous experiments, the carriers were illuminated through a mask with monochromatic radiation (447 nm) at 45 mW/cm^2 incident power. Thermoplastic visualization was carried out under the same conditions as X-rays imaging. The images with a good contrast were obtained at an exposure power of 230 mJ/cm^2.

The following experiments were carried out by use of smaller diameter wires. Fig.3 shows the X-ray image of the 6 µm (diameter) tin wire.

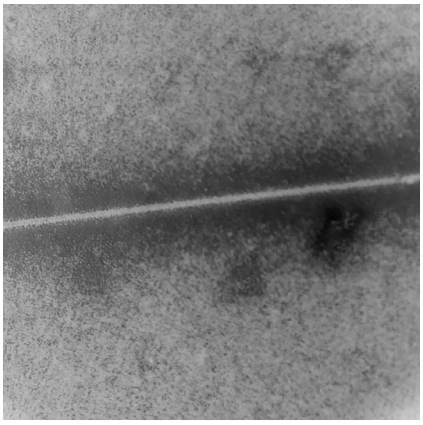

Fig.3 X-ray image of the tin wire with a diameter of 6 µm recorded at an absorbed dose of 1,78 Gy.

The image was recorded using the continuous spectrum of X-rays tungsten tube (absorbed dose 1,78 Gy). Thermoplastic visualization (Fig.1b) was carried out at a temperature of 78^0C and charging time t=2,4 s. The visualization was followed by a study on the images by use of optical microscope in reflected light (magnification of 1200^x). The 6 µm (diameter) wire was the smallest object which could be recorded in these investigations. A part of the image was investigated using the AFM (Fig.4).

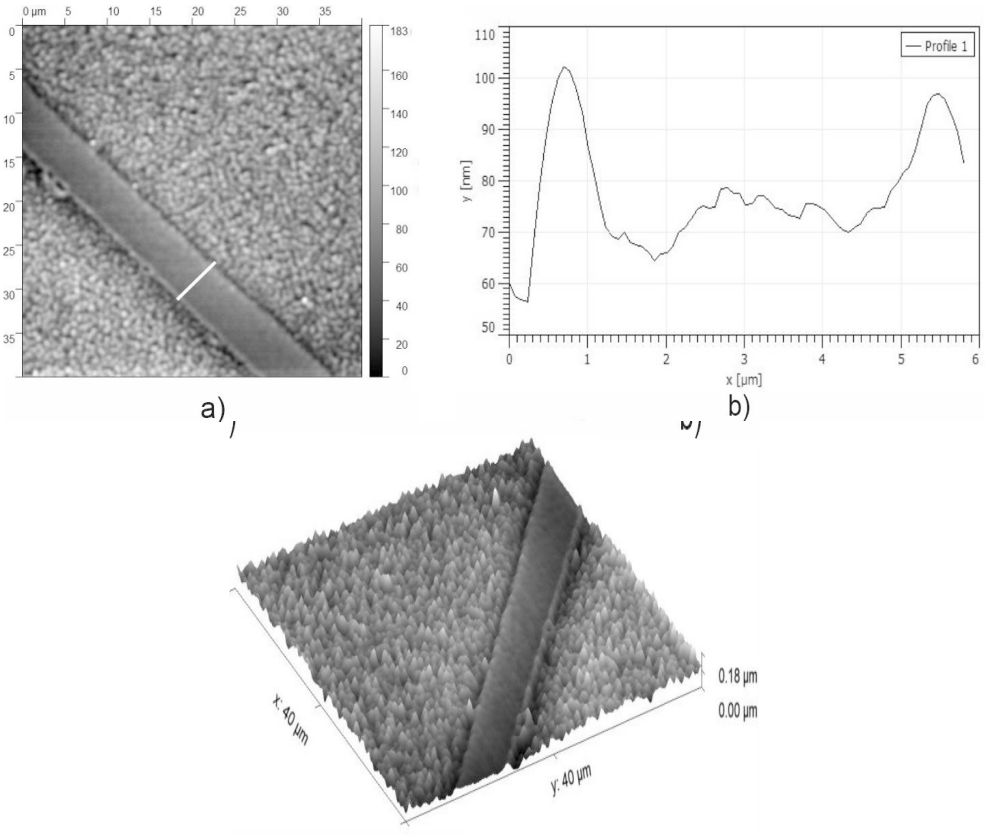

Fig. 4. AFM image of the tin wire with a diameter of 6 µm.

The AFM image shows the presence of the thermoplastic layer deformation in irradiated areas and the absence of deformation in the non-irradiated ones (Fig.4a). The surface profile

(white line Fig.4a) shows a 30 nm average depth between irradiated and non-irradiated areas (Fig.4b). Fig.4c shows a three-dimensional image of the selected area with deformation in the irradiated areas and no deformation in the non-irradiated ones.

The effect of photostructural changes (photodarkening, photorefraction) in chalcogenide glassy semiconductors under optical radiation is well known from different references [1, 23–24]. This effect was not observed during the X-ray irradiation of the investigated carriers. Measurement of the optical transmission spectral dependence before and after X-ray irradiation at an absorbed dose up to 1,78 Gy showed no changes in the transmission of the investigated samples.

4. Discussions

The investigations carried out showed the presence of sensitivity of the chalcogenide glassy semiconductors of the 67at%$(As_2S_3)_{0,985}(Bi_2Se_3)_{0,015}$:33at.% As_2Se_3 system to X-rays for imaging use. The deformation of the thermoplastic layer in the irradiated areas takes place under irradiation by a continuous spectrum of tungsten X-ray tube. This indirectly indicates the presence of structural changes in the semiconductor layer under X-ray irradiation, the latter causing the semiconductor layer' resistivity modulation [16-17]. However, no change in the optical transmittance in the 67at%$(As_2S_3)_{0,985}(Bi_2Se_3)_{0,015}$:33at.% As_2Se_3 layer under X-rays irradiation at an absorbed dose of 1,8 Gy (continuous spectrum tungsten anode tube) was detected. One can note, that similar results were presented as well in [16-17] for chalcogenide glassy semiconductors of the As-Se-S system doped by Sn and Te. Some changes in the optical properties of CGS was found under the γ-radiation [25–26], but the darkening of the layers of As-S was observed under hard γ-quanta (1,25 MeV) irradiation and at high radiation doses - up to 10 MGy [25–26].

The resolution power of photothermoplastic carriers based on the polyepoxypropylcarbazole/As-Se-S structure reaches values up to 4000 mm^{-1} [11]. It was not possible to register an X-ray image of a wire smaller than 6 μm in diameter (in given experiments). Thermoplastic visualization of X-ray images of *W* wires with diameters of 30 μm was carried out at temperature T=78^0C and charging time of 3,2 s. The average depth between irradiated and non-irradiated areas (0,1 μm) was obtained (Fig.2c). The thermoplastic visualization of X-ray images of tin wire with diameter of 6 μm was carried out at 78^0C and charging time of 2,4 s. he average depth in-between irradiated and non were just 30 nm (Fig.4b). An increase in the charging time more than 2,4 s, causes a complete loss of the image sharpness. The deformation occurred both in irradiated and non-irradiated places. However, a high resolution in optical recording [11] was obtained for a high-contrast interference pattern formed by plane-parallel monochromatic laser beams. In the carried out experiments, the contact registering method was used, which considers the wire (as a mask for X-ray recording) to be placed onto the surface of the thermoplastic layer. By use of this design, the wire is 0,6 μm (thermoplastic layer thickness) from the semiconductor layer (Fig.1a). Unlike the optical recording [11] a wide spectral range of X-rays ("white" spectrum a tube with a *W* anode) is used for images recordings in this work. Also, the X-ray beam is not perfectly parallel, as in the holographic recording. It can be assumed that these factors partially influenced the X-ray recording process.

5. Conclusions

The polyepoxypropylcarbazole/ 67at%$(As_2S_3)_{0,985}(Bi_2Se_3)_{0,015}$:33at.% structure makes it possible to record X-ray images using the continuous spectrum of X-ray tube with tungsten anode and laser radiation with a wavelength of 447 nm.

It was possible to register an X-ray image of a tin wire with a diameter of 6 μm at this stage of research. It can be assumed that this is not the limiting resolution of the polymer/chalcogenide glassy semiconductor structure. It was not technically possible to use a

well-collimated X-ray beam in these studies. The resolution power of the polyepoxypropylcarbazole/ 67at%$(As_2S_3)_{0,985}(Bi_2Se_3)_{0,015}$:33at.% structure (as well as similar structures based on As-Se-S doped with Sn and Te [16-17]) requires more detailed studies, which is the goal of further research.

Acknowledgements

This research was funded by the National Agency for Research and Development of the Republic of Moldova, grant 20.80009.5007.12

References

[1] E. Achimova, A. Stronski , V. Abaskin, A. Meshalkin, A. Paiuk, A. Prisacar, P. Oleksenko, G. Triduh, Optical Materials 47, 566 (2015); https://doi.org/10.1016/j.optmat.2015.06.044
[2] V. Cazac, A. Meshalkin, E. Achimova, V. Abashkin, V. Katkovnik, I. Shevkunov, D. Claus, and G. Pedrini, Applied Optics 57, 507 (2018); https://doi.org/10.1364/AO.57.000507
[3] M. Iovu, S. Sergeev, O. Iaseniuc, Optoelectron. Adv. Mat. 12(7-8), 377 (2018)
[4] A. O. Iaseniuc, M. Enachescu, D. Dinescu, M. Iovu, S. Sergheev, J. Optoelectron. Adv. M. 18(1-2), 34 (2016)
[5] S. Sergeev, M. Iovu, A. Meshalkin, Chalcogenide Letters 17(1), 25 (2020)
[6] O. Iaseniuc, I. Cojocaru, A. Prisacar, A. Nastas, M. Iovu, Journal of Optics and Spectroscopy 121(1), 1128 (2016); https://doi.org/10.1134/S0030400X16070237
[7] A. Nastas, A. Andriesh, V. Bivol, A. Prisakar, G. Tridukh, Technical Physics Letters 32(1), 45 (2006); https://doi.org/10.1134/S1063785006010159
[8] A. Nastas, A. Andriesh, V. Bivol, A. Prisakar, G. Tridukh, Technical Physics 54(2), 305 (2009); https://doi.org/10.1134/S1063784209020236
[9] J. Teteris, M. Reinfelde, Journal of Optoelectronics and Advanced Materials 5(5), 1355 (2003)
[10] A. Chirita, N. Kukhtarev, T. Kukhtareva, O. Korshak, V. Prilepov, Journal of Modern Optics 59(16), 1428 (2012); https://doi.org/10.1080/09500340.2012.719936
[11] A. Chirita, N. Kukhtarev, T. Kukhtareva, O. Korshak, V. Prilepov, Laser Physics 23, 036002 (2013); https://doi.org/10.1088/1054-660X/23/3/036002
[12] I. Andries, T.Galstian, A.Chirita, J. Optoelectron. Adv. M. 18(1-2), 56 (2016)
[13] A. Chirita, V. Prilepov, M. Popescu, I. Andries, M. Caraman, Iu. Jidcov, J. Optoelectron. Adv. M. (7-8), 925 (2015)
[14] G. Danev, E. Spassova, J. Assa, P. Guttmann, Advanced materials for optics and electronics 8, 129 (1998); https://doi.org/10.1002/(SICI)1099-0712(199805/06)8:3<129::AID-AMO331>3.0.CO;2-5
[15] A. Buroff, A. Rush, Journal of Non Crystalline Solids 90, 585 (1987); https://doi.org/10.1016/S0022-3093(87)80491-X
[16] A. Chirita, V. Prilepov, Chalcogenide Letters 19(6), 439 (2022), https://doi.org/10.15251/CL.2022.196.439
[17] A.Chirita, D.Spoiala, S.Vatavu, Chalcogenide Letters 19(10), 683 (2022) https://doi.org/10.15251/CL.2022.1910.683
[18] V. Prilepov, M. Popescu, A. Chirita, O. Korshak, P. Ketrush, N. Nasedchina. Chalcogenide Letters 10(7), 249 (2013)
[19] A. Chirita, V. Prilepov, M. Popescu, O. Corsac, P. Chetrus, N. Nasedchina. Optoelectron. Adv. Mat. 9(7-8), 919 (2015)
[20] A.Nastas, A. Andriesh, V. Bivol, I. Slepnev, A. Prisakar, Technical Physics Letters 35(4), 375 (2009); https://doi.org/10.1134/S1063785009040269
[21] A. Chirita, T. Galstian, M. Caraman, V. Prilepov, O. Korshak, I. Andries, Optoelectron. Adv. Mat. 7(3-4), 293 (2013)
[22] A. Chirita, F. Dimov, S. Pradhan, P. Bumacod, O. Korshak, Journal of Nanoelectronics and Optoelectronics 7(4), 415 (2012); https://doi.org/10.1166/jno.2012.1321

[23] J. De Neufville, S. Moss, S. Ovshinsky, Journal of Non-Crystalline Solids 13, 191(1973); https://doi.org/10.1016/0022-3093(74)90091-X
[24] T. Uchino, D. Clary, Physical Review Letters 85(15), 3305 (2000); https://doi.org/10.1103/PhysRevLett.85.3305
[25] O. Shpotyuk, A. Matkovskii, Journal of Non-Crystalline Solids 176, 45 (1994); https://doi.org/10.1016/0022-3093(94)90209-7
[26] M. Shpotyuk, A. Kovalskiy, R. Golovchak, O. Shpotyuk, Journal of Non-Crystalline Solids 498, 315 (2018); https://doi.org/10.1016/j.jnoncrysol.2018.04.006